Geoderma 232–234 (2014) 130–140

Contents lists available at ScienceDirect

Geoderma

journal homepage: www.elsevier.com/locate/geoderma

Mercury distribution in a toposequence of sub-Antarctic forest soils of Tierra del Fuego (Argentina) as consequence of the prevailing soil processes

Susana Peña-Rodríguez [a], Xabier Pontevedra-Pombal [b], Eduardo García-Rodeja Gayoso [b], Alicia Moretto [c,d], Romina Mansilla [c], Laura Cutillas-Barreiro [a], Manuel Arias-Estévez [a], Juan Carlos Nóvoa-Muñoz [a,*]

[a] Área de Edafología y Química Agrícola, Facultad de Ciencias, Universidad de Vigo, As Lagoas s/n, 32004 Ourense, Spain
[b] Departamento de Edafología y Química Agrícola, Facultad de Biología, Universidad de Santiago, Rúa Lope Gómez de Marzoa s/n, 15782 Santiago, Spain
[c] Centro Austral de Investigaciones Científicas (CADIC-CONICET), Bernardo Houssay 200, 9410 Ushuaia, Tierra del Fuego, Argentina
[d] Universidad Nacional de Tierra del Fuego, Onas 450, 9410 Ushuaia, Tierra del Fuego, Argentina

ARTICLE INFO

Article history:
Received 29 July 2013
Received in revised form 14 February 2014
Accepted 23 April 2014
Available online xxxx

Keywords:
Sub-Antarctic forest soils
Mercury
Podzolization
Polycyclism
Non-crystalline Al and Fe compounds

ABSTRACT

The total content, distribution and assessment of Hg sources in five soils of a toposequence of sub-Antarctic forest soils in Tierra del Fuego were explained as a combination of pedogenetic processes and the interactions between Hg and the soil compounds. The soils of the toposequence were mainly podzols and podzolic soils, strongly acidic (water pH < 5.0), organic matter rich in O horizons (239–444 g kg^{-1}) and non-crystalline compounds dominate Al and Fe distribution. The total Hg (Hg_T) values ranged between 12 and 375 ng g^{-1} and diminished with soil depth although the secondary peaks of the Hg_T were observed in illuvial (Bhs or Bs) or buried A horizons. The total Hg was significantly correlated to the total contents of C, N and S ($r > 0.71$) and to the contents of the non-crystalline Al and Fe compounds (0.44–0.71), whereas the Hg/C ratio increases with soil depth up to values of 11.3 μg Hg g^{-1} C. Exogenic Hg, i.e. Hg deposited from the atmosphere (Hg_{Exo}), constitutes over 87% of the Hg_T in the O and A horizons, whilst lithogenic Hg (Hg_{Lit}) is 36% of the average Hg_T.

Podzolization seems to control the distribution of the Hg_T in the mid-slope and upslope soils (P480, P590, P630), as suggested by the Hg_T peaks in the Bhs or Bs horizons, where illuviated organic matter and non-crystalline Al and Fe compounds favour Hg retention. In the downslope soils (P340 and P220), both podzolization and polycyclism (that result in soils formed by two or more different and contrasting processes derived from a substantial change in soil formations factors, that lead to the accumulation of features over their lifetime), seem to influence the Hg_T depth pattern in light of the high values observed in the A and Bhs horizons of the buried soils. The significant correlation between the Hg/C and C_p/C ratios strengthens the efficiency of humified organic matter to complex Hg, whereas the peaks of the Hg/C ratio in the Bhs and Bs horizons also indicate that Al and Fe compounds are also involved in Hg retention.

Polycyclic events, i.e. those contrasting soil processes that lead to different chemical and morphological signatures within the soil profile, could justify high Hg_{Lit} values in the deeper horizons of the downslope soils, whilst the peaks of Hg_{Exo} in the Bhs or Bs horizons could be considered to be a consequence of Hg mobilization and the subsequent retention by Al and Fe compounds during podzolization which is supported by the significant correlations of these soil compounds with Hg_{Exo}.

Environmentally, illuvial horizons and buried A horizons could act as a safety mechanism delaying the arrival of Hg to stream waters.

1. Introduction

Mercury is considered to be a global pollutant, because it can be dispersed and transported in the atmosphere worldwide (Schroeder and Munthe, 1998). Mercury reaches soil surface predominantly through wet and dry deposition and litterfall (Munthe et al., 1995; St. Louis et al., 2001). Thus, soils can accumulate up to 75% of the Hg present in the biosphere (Mason and Sheu, 2002), mostly as a result of the affinity of Hg for soil organic matter and Al and Fe oxyhydroxides (Schuster,

Abbreviations: CCT, Cerro Castor toposequence; Al_{ed}, Fe_{ed}, Mn_{ed}, Cu_{ed}, Zn_{ed}, Al, Fe, Mn, Cu and Zn extracted with Na_2-EDTA + NH_4OAc; Al_p, Fe_p, Al and Fe extracted with Na-pyrophosphate; Al_o, Fe_o, Al and Fe extracted with ammonium oxalate–oxalic acid; Al_n, Al extracted with Na-hydroxide; Fe_d, Fe extracted with Na–dithionite–citrate; C_p, Na-pyrophosphate extractable C; Hg_T, total mercury; Hg_{Lit}, lithogenic Hg; Hg_{Exo}, exogenic Hg; Hg_{TRes}, areal mass of total Hg stored in soil horizons.

* Corresponding author. Tel.: +34 988 387070; fax: +34 988 387001.
E-mail address: edjuanca@uvigo.es (J.C. Nóvoa-Muñoz).

http://dx.doi.org/10.1016/j.geoderma.2014.04.040
0016-7061/

1991; Skyllberg et al., 2006). Soils are not exclusively a sink of Hg, as volatilization of Hg^0 from soil surface and exports of ionic Hg to surface waters by leaching have been recognized (Gustin et al., 2006).

The presence of Hg species in surface waters is of particular concern for human health and wildlife (Clarkson and Magos, 2006). As a consequence, the biogeochemical behaviour of Hg in soils was intensively studied during the last few decades, primarily in the surroundings of anthropogenic Hg sources (Glodek and Pacyna, 2009; Rothenberg et al., 2010). In contrast, the fate of Hg in soils with low or natural background concentrations (<100 ng g^{-1}) is still limited, despite their notable influence on the global Hg cycle due to the large areas they cover (Gustin et al., 2008). Moreover, even pristine soils exhibit total Hg contents of up to 500 ng g^{-1} (Grimaldi et al., 2008; Guedron et al., 2006), exceeding the threshold value of 130 ng g^{-1} established as the critical load for Hg in soils (Tipping et al., 2010). Thus, it becomes necessary to study the geochemical behaviour of Hg in non-polluted soils, because the relationship between soil processes and their components with Hg could be useful to deal with environmental consequences under scenarios of high Hg deposition.

Studies on the fate of Hg in terrestrial ecosystems have been mostly performed in forested areas from the boreal and temperate zones of the northern hemisphere, where the total Hg distribution in soils is characterized by its accumulation in the uppermost soil horizons which is associated to organic matter (Demers et al., 2007; Meili, 1991), whilst the deeper soil layers are often Hg enriched as a consequence of its transport as metal–humus complexes during podzolization (Alriksson, 2001; Johansson et al., 1991; Schwesig and Matzner, 2000).

Abnormally high values of the total Hg in pristine soils were reported in both tropical and equatorial zones (De Oliveira et al., 2001), although Hg was also mobilized due to land use changes and artisanal gold mining (Roulet et al., 1998). The mercury distribution in the surface horizons of tropical and equatorial soils depends on atmospheric deposition (Guedron et al., 2006), whereas in the deeper soil layers Hg is controlled by carrier phases such as organic matter, clay, and Fe and Al oxyhydroxides, which are closely related to pedogenetic processes (Do Valle et al., 2005; Fiorentino et al., 2011; Grimaldi et al., 2008; Guedron et al., 2009; Roulet et al., 1998).

Little is known about the behaviour of Hg in non-polluted forest soils at the high latitudes of the southern hemisphere, in spite of the fact that the global distillation effect could favour the transport of atmospheric Hg towards these latitudes as it occurs in the northern hemisphere. The existing studies describe a soil Hg distribution closely associated with organic matter (Hermanns and Biester, 2011) or with organic matter/water circulation system (Bargagli et al., 2007), whereas Hg contamination could have occurred during gold exploitation in the soils of the northeast areas of Tierra del Fuego (Bascopé, 2010).

In the forested areas of Tierra del Fuego (southernmost South America), the lowlands are primarily covered by peatlands, whose role as a source of methyl-Hg to surface waters is well known (Mitchell et al., 2008). These sources of Hg highlight the need to study the geochemical fate of Hg in a toposequence of the non-polluted upland soils of sub-Antarctic deciduous forests from Tierra del Fuego. To accomplish such a study, the total Hg content and the background values were quantified in a soil toposequence to: 1) explain its distribution with soil depth as a function of the main pedogenetic processes in the toposequence and 2) determine the role of soil components in Hg retention. Finally, for a better understanding of Hg the behaviour in the studied upland soils, Hg originating from lithological and atmospheric sources was discriminated using Ti as a conservative element.

2. Material and methods

2.1. Study area and soil sampling

The study area is located in the Isla Grande de Tierra del Fuego at the southernmost tip of South America (53–55° S and 66–74° W; Fig. 1). The landscape is dominated by the Fuegian Andes (<1500 m a.s.l.) and it is characterized by very steep slopes and large glacial valleys that are covered by peatlands. The climate is cold-temperate (mean annual temperature in the range of 5–6 °C and 550 mm/year of rainfall), and the vegetation consists of sub-Antarctic deciduous forests primarily composed of lenga beech (*Nothofagus pumilio* Poepp. & Endl). Sedimentary rocks (mudstones and lutites), schists rich in quartz veins, phyllites and slates are the main lithological material of the area (Olivero and Martinioni, 2001), which are frequently covered by fine-matrix till deposits, whose formation was due to an intense glacial activity. Soils are shallow, with thick organic horizons and evidence of podzolization, with leptosols, umbrisols, cambisols and podzols being the most frequent soil types in the mountain slopes, whereas histosols cover the valley bottoms and the footslopes (Godagnone and Irisarri, 1990).

The study site is a toposequence of lenga beech forest soils located at the south-facing slope of the Cerro Castor (54°43′ S, 68°00′ W) near the city of Ushuaia (Fig. 1). The Cerro Castor toposequence (hereinafter denoted as CCT) has slopes that range from 10% to 27%, and five sites were selected and named as P630, P590, P480, P340 and P220 according to their altitudes in metres above sea level. In each site, a 1.5-m long trench was dug with a shovel down to the parent material. Samples from the identified soil horizons were collected using a garden-trowel and immediately double-bagged in plastic bags, stored at 4 °C and transported to the laboratory. Thick soil horizons were split into several soil samples, whilst maintaining the depth sequence. A sample of the parent material of each soil was also collected for the characterization of its geochemical background.

The upslope and mid-slope soils (P630, P590 and P480) exhibit a similar morphology, being shallow (C horizon occurs at 26 cm depth), developed from glacial till, with a sequence of horizons beginning with a carbon rich organic horizon followed by a whitish E horizon and a reddish Bs or Bhs horizon, whereas the C horizons exhibit some signs of temporal reducing conditions. The downslope soils (P340 and P220) are thicker, with less perceptible whitish or reddish horizon and evidence of colluviums and buried soils; the oldest soil cycle was developed from schists.

2.2. Soil analysis

The chemical characterization of the soils was performed on the air-dried fine earth fraction (<2 mm). The particle-size distribution, distinguishing between sand (0.05–2 mm), silt (0.02–0.05 mm) and clay (<0.002 mm) fractions, was determined by the internationally-recognized pipette method. The soil pH in water (pH_w) and 0.1 M KCl (pH_k) solutions were measured at a soil/solution ratio of 1:2.5. The total contents of carbon, nitrogen and sulphur were determined by elemental analyzers using finely-milled soil samples. The cation exchange capacity at the soil pH (eCEC) was estimated as the sum of the base cations (K, Na, Ca, Mg) in 1 M NH_4Cl (Peech et al., 1947) and the Al extracted with 1 M KCl (Bertsch and Bloom, 1996). The available metals (Al_{ed}, Fe_{ed}, Mn_{ed}, Cu_{ed} and Zn_{ed}) were determined after extraction with 0.02 M Na_2-EDTA + 0.5 M NH_4OAc solution buffered at pH 4.65 (Lakenen and Ervio, 1971).

The aluminium and Fe distribution in the solid phase of the soil was determined following the procedures used by García-Rodeja et al. (2007). Briefly, a 0.1 M Na-pyrophosphate solution was used to estimate the total content of metal (Al, Fe)–humus complexes (Al_p, Fe_p), whereas 0.2 M ammonium oxalate–oxalic acid buffered at pH 3 dissolves, in addition to organically-bound Al and Fe, inorganic non-crystalline hydrous oxides of both metals (Al_o, Fe_o). The amount of carbon solubilised in the Na-pyrophosphate (C_p) extracts was also determined for the mineral soil horizons. A 0.5 M NaOH solution was used to estimate the total free Al pool (Al_n), including Al from gibbsite and poorly ordered 1:1 phyllosilicates. Sodium–dithionite–citrate was used to assess the total free Fe (Fe_d), which includes non-crystalline Fe

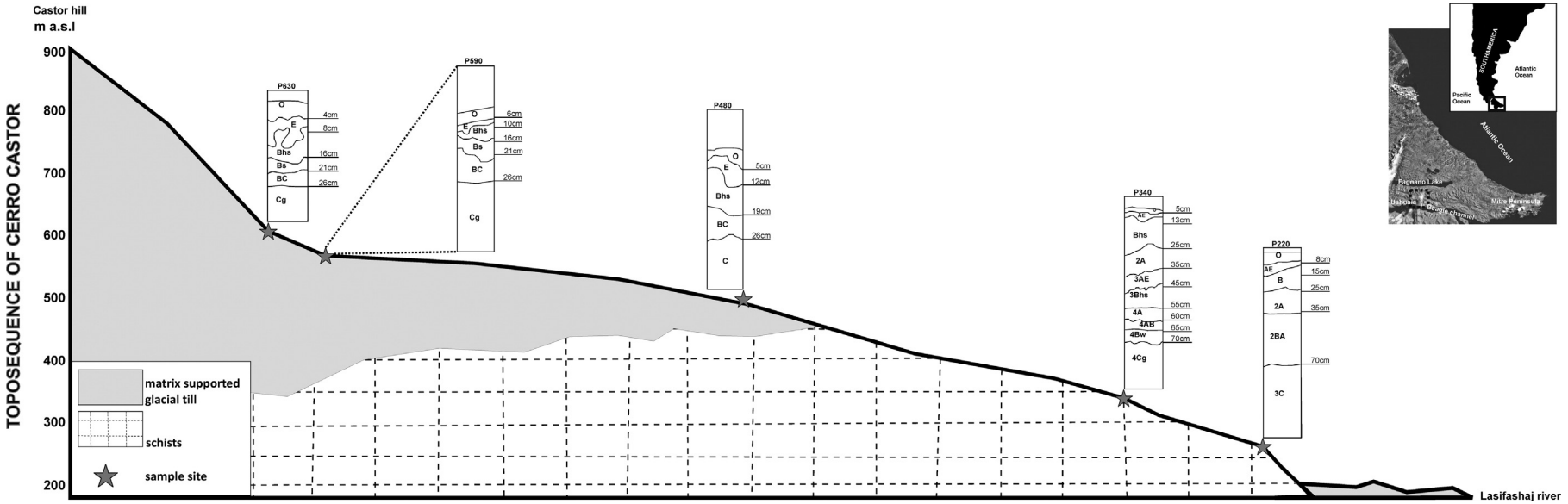

Fig. 1. Location of the study area in Tierra del Fuego (top right squares) and the distribution of the studied soils in the toposequence of the Cerro Castor (CCT) showing the pedological horizons and their depths.

(organic and poorly ordered inorganic Fe) and Fe dissolved from crystalline oxy-hydroxides.

The metal concentration in all extracts was analyzed by flame atomic absorption (or emission) spectroscopy.

2.3. Total mercury analysis

The total mercury (Hg_T) concentrations in finely milled soil samples were determined by atomic absorption spectroscopy after thermal combustion using a Nippon Model MA-2000 total Hg analyzer. The analyzer was calibrated using 0.01 mg L^{-1} and 0.1 mg L^{-1} of Hg stock solutions made from 1000 mg L^{-1} $HgCl_2$ standard in 0.001% L-cysteine. The analyzer has a detection limit of 0.002 ng and a working range of 0.002–1000 ng, both expressed as the absolute amount of Hg. The soil mass used for Hg analysis ranged from 50 to 200 mg.

All soil and parent material samples were analyzed in duplicates, and the analyses were repeated when the coefficient of variation exceeded 10%. Standard reference materials of the National Institute of Standards and Technology (NIST-1547, peach leaves, 31 ± 7 ng g^{-1} Hg), the National Research Council Canada (NRC MESS-3, estuarine sediment, 91 ± 9 ng g^{-1} Hg) and a reference material approved by China National Analysis Center for Iron and Steel (NCS DC73323, soil, 290 ± 30 ng g^{-1} Hg) were measured at the beginning of each analytical run and repeated every ten samples. When the deviation of the Hg values of the standard materials was higher than 5%, the Hg-analyzer was recalibrated, and the soil samples analyzed since the last satisfactory values of standards were re-analyzed. All the mercury values are expressed as the oven-dry weight (105 °C).

The areal mass of total Hg, i. e. the soil reservoir of Hg_T (Hg_{TRes}), is the sum of the Hg_T accumulated in the corresponding soil layers, which is calculated using the thickness of the horizon, its bulk density and Hg_T concentration as it is shown in Eq. (1).

$$Hg_{TRes} = BD * Hg_T * P \quad (1)$$

where Hg_{TRes} is the reservoir of total Hg in a soil horizon (in mg Hg_T m^{-2}), whereas BD, Hg_T and P are the soil bulk density (in Mg m^{-3}), the total Hg (in mg Hg Mg^{-1} soil) and the soil depth (in m) for each soil horizon, respectively.

2.4. Calculation of lithogenic and exogenic Hg in the soil profiles

Mercury derived from the weathering of the soil parent material, lithogenic Hg (Hg_{Lit}), can be discriminated from those deposited from the atmosphere, exogenic Hg (Hg_{Exo}), following the approach used by Hissler and Probst (2006) and Guedron et al. (2006). In this approach, Hg_{Lit} was estimated through Eq. (2) after normalising the total Hg values to the concentrations of a conservative element that is not significantly influenced by atmospheric sources, such as Ti, which was determined by X-ray fluorescence in finely milled soil and parent material samples.

$$[Hg_{Lit}] = [k]_u * \left([Hg]_d/[k]_d\right) \quad (2)$$

where k is the reference element (i.e. Ti), the subscript u refers to each soil horizon and the subscript d refers to the soil parent material. The brackets indicate mean concentrations in g kg^{-1} (for Ti) and μg kg^{-1} (for Hg).

Exogenic Hg (Hg_{Exo}), which includes all Hg contributions except those from lithological sources, is estimated by subtracting Hg_{Lit} from the total Hg (Eq. (3)).

$$[Hg_{Exo}] = [Hg_T]\text{-}[Hg_{Lit}] \quad (3)$$

where Hg_T is the total Hg content in each soil horizon. The square brackets indicate concentrations in μg kg^{-1}.

2.5. Statistical analysis

Because most geochemical data are not normally distributed, Spearman's rho correlations (Elliot and Woodward, 2007) were applied to relate the total, lithogenic and exogenic Hg contents with the common soil characteristics. Moreover, a non parametric Kruskal–Wallis test (Elliot and Woodward, 2007) was used to assess the heterogeneity of the Hg_T pattern with soil depth by grouping their values based on the type of horizon. The results were considered significant at a probability level of $P = 0.05$. All statistical analyses were performed using the Statistical Package for the Social Sciences (SPSS 17.0, SPSS Inc. Chicago, IL).

3. Results

3.1. General characteristics of soils

In general terms, the soils from the CCT are mainly podzols and podzolic soils, with a particle size distribution primarily dominated by the sand fraction (range 30–77%, Fig. 2). The soil textures are loam to sandy-loam in the soils P480, P590 and P630, and finer (silty-loam, clay-loam or sandy clay) in the soils P220 and P340. The chemical characteristics of the CCT soils are listed in Table 1 (more details are available in supplementary Table S1).

The uppermost horizons of the upslope and mid-slope soils of the CCT (P480, P590 and P630) are strongly acidic ($pH_w > 4.2$), increasing with depth up to values around 5.0 in C horizons (Table 1). The soils P220 and P340 are considerably less acidic and pH_w values are always above 5.5. Eluvial horizons (E) exhibited the lowest pH values in saline solution ($pH_k < 3.2$), whereas ΔpH (i.e., $pH_w - pH_k$) indicates a notable presence of exchangeable Al in the strongly acidic soils.

Because these soil pH values exclude the presence of carbonates in the soils of the CCT, the total C is entirely organic in nature, and it decreases with soil depth, from values greater than 238 g kg^{-1} in the O horizons to those lower than 15.8 g kg^{-1} in the deeper soil layers, although all soils of the CCT exhibited subsurface peaks of organic C (Table 1). The total N and S exhibited a similar trend to that of organic C, being higher in organic (>11 and 2 g kg^{-1}, respectively) than in mineral horizons (ranges 0.8–3.6 g kg^{-1} for N and 0.2–0.6 g kg^{-1} for S). The effective cation exchange capacity (eCEC) exceeds 25 $cmol_c$ kg^{-1} in the organic horizons, in which Ca is the dominant exchangeable cation (Table 1). In the CCT soils, the eCEC decreases with depth to less than 10 $cmol_c$ kg^{-1} in the deeper horizons, which also exhibit high Al saturation (>80%), especially in the upslope and mid-slope soils.

The non-crystalline compounds dominate the distribution of Al and Fe in the soil solid phase, with the mean values of Al_o/Al_n and Fe_o/Fe_d ratios being 1.1 and 0.6, respectively. Organically-bound Al and Fe are prevalent in the Bhs horizons of the upslope and mid-slope soils, whose ranges are 3.6–10.0 and 7.5–18.9 g kg^{-1}, respectively (Table 1). Organically-complexed Fe (Fe_p) also dominated the Fe distribution in the downslope soils (P220 and P340). Inorganic non-crystalline Al (i.e., $Al_o - Al_p$) only appeared in significant amounts in soil P340, whereas the equivalent Fe compounds ($Fe_o - Fe_p$) prevailed over the Fe–humus complexes in the O and C horizons. The lowest values of non-crystalline Al or Fe compound are found in the E horizons of soils P480, P590 and P630 (Table 1).

The lower values of Ti are found in the organic horizons of all soils, and the Ti levels do not show significant changes with soil depth except in the soil P220. In the soil parent material, the Ti values range from 1.9 g kg^{-1} in the downslope soils (developed from schists) to approximately 5.0 g kg^{-1} in the mid-slope and upslope soils derived from glacial till.

3.2. Total mercury content and distribution in soil profiles

The total Hg (Hg_T) values in the soils of the CCT ranged from 12 to 375 ng g^{-1}, decreasing gradually with depth from the organic horizons

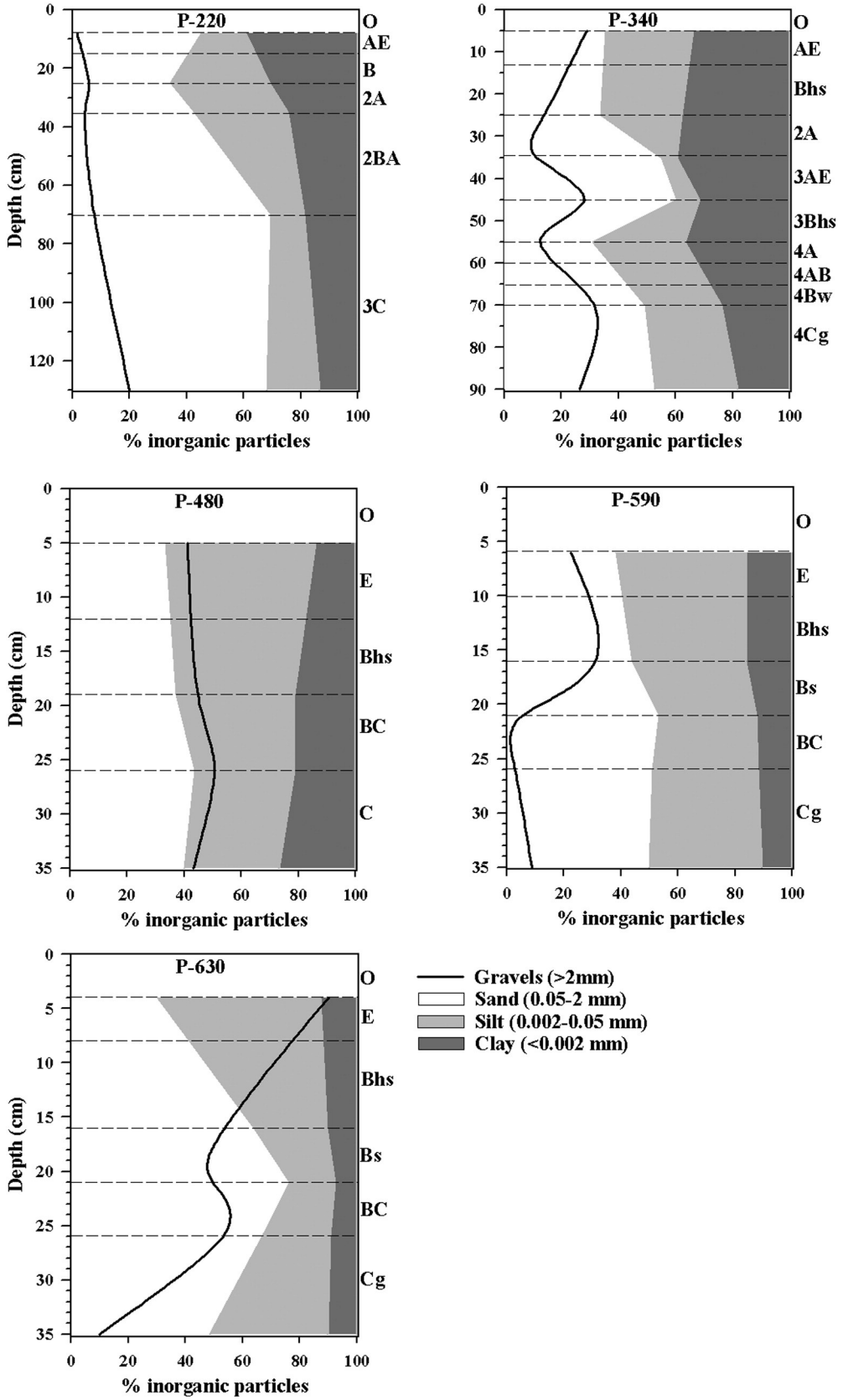

Fig. 2. Distribution of the particle size fractions as relative percentages of the fine earth (<2 mm) and the mass percentage of the coarse elements (>2 mm) for each profile of the Cerro Castor toposequence.

Table 1
Chemical characteristics of the soil profiles sampled in the Cerro Castor toposequence.

Soil	Hor	Depth	n[a]	pH_w[b]	pH_k[b]	C	N	S	SB[c]	eCEC[c]	sAl[c]	Al_p[d]	Al_o[d]	Al_n[d]	Fe_p[d]	Fe_o[d]	Fe_d[d]	Ti
		cm				g kg^{-1}			cmol$_c$ kg^{-1}		%	g kg^{-1}						
P-220	O	0–8	2	5.4	5.1	238.5	11.3	1.5	40.9	41.3	0.4	1.5	2.0	1.3	5.8	9.3	13.2	7.4
	AE	8–15	1	5.7	4.9	28.2	2.1	0.4	12.2	12.5	1.0	2.3	3.8	2.8	10.3	17.4	25.4	13.8
	B	15–25	2	5.5	4.1	18.6	1.1	0.3	5.8	9.2	14.8	2.9	4.0	4.0	11.5	17.5	24.9	17.6
	2A	25–35	2	5.6	4.2	17.0	0.8	0.3	3.5	5.9	17.3	4.2	6.0	6.1	11.8	16.1	23.8	18.1
	2BA	35–70	4	5.7	4.3	7.6	<0.8	0.2	1.6	2.3	32.3	2.4	3.2	3.5	4.2	5.6	12.2	15.5
	3C	70–130	3	5.5	4.6	3.0	<0.8	0.2	0.5	0.8	36.6	1.2	2.9	3.0	0.5	2.8	9.5	9.6
P-340	O	0–5	1	5.2	4.8	264.6	10.6	1.4	38.2	38.6	0.1	0.7	1.0	0.7	1.9	3.0	5.0	4.3
	AE	5–13	1	4.6	3.6	32.6	1.9	0.3	1.2	9.4	42.0	2.8	4.4	4.8	9.3	14.2	21.4	8.8
	Bhs	13–25	2	4.9	3.9	36.2	1.6	0.3	0.6	7.2	41.4	7.7	9.9	10.2	12.9	19.2	23.6	9.7
	2A	25–35	2	5.4	4.5	32.6	1.6	0.3	2.1	3.1	32.4	8.8	12.1	12.0	23.5	39.3	48.2	10.0
	3AE	35–45	2	6.0	5.4	33.4	2.1	0.5	8.5	8.6	0.9	7.4	12.9	11.1	17.7	38.7	48.2	8.3
	3Bhs	45–55	2	6.2	5.8	42.3	3.3	0.9	9.7	9.7	<0.1	9.0	18.7	13.9	10.7	21.9	30.2	8.4
	4A	55–60	1	6.1	5.8	44.8	3.6	0.9	9.0	9.0	<0.1	10.0	20.0	16.5	10.2	18.8	26.3	8.2
	4AB	60–65	1	6.3	5.7	34.8	2.8	0.7	8.3	8.3	<0.1	7.7	16.0	15.1	7.8	15.0	21.2	9.1
	4Bw	65–70	1	6.4	5.8	20.3	1.6	0.5	6.2	6.2	<0.1	4.5	10.6	7.9	4.6	7.6	12.0	9.7
	4Cg	70–90	2	6.4	5.8	7.9	<0.8	0.3	3.1	3.1	<0.1	2.0	3.7	4.4	1.8	2.4	5.2	8.5
P-480	O	0–5	1	3.9	3.4	395.3	12.2	2.6	24.2	30.6	1.9	1.1	1.3	1.1	0.9	1.9	2.7	2.3
	E	5–12	1	4.1	3.2	13.0	0.8	0.2	0.5	8.9	38.8	0.9	1.7	1.1	1.0	1.6	3.3	6.0
	Bhs	12–19	1	4.6	4.0	25.4	1.3	0.3	0.5	5.6	41.3	3.6	6.9	4.6	18.9	43.4	48.0	10.9
	BC	19–26	1	4.6	4.1	17.7	0.9	0.2	0.3	1.3	77.1	2.8	3.9	4.5	9.7	15.9	30.8	7.8
	C	>26	1	4.6	4.1	15.8	0.8	0.3	0.3	1.6	80.2	2.9	3.5	4.4	9.1	15.0	28.4	7.3
P-590	O	0–6	1	4.0	3.2	375.9	13.3	2.3	16.0	25.1	6.7	2.0	2.6	2.4	0.9	2.5	4.1	2.7
	E	6–10	1	4.1	2.9	35.4	1.8	0.2	0.7	9.6	38.5	1.1	1.4	1.4	1.2	2.2	5.4	7.7
	Bhs	10–16	1	4.6	3.5	45.2	2.5	0.4	0.3	8.1	38.7	4.0	4.7	5.1	11.7	21.1	26.7	8.2
	Bs	16–21	1	4.6	4.0	19.8	0.9	0.2	0.1	6.3	32.2	3.9	4.5	5.2	9.8	12.0	21.2	7.9
	BC	21–26	1	4.8	4.3	7.6	<0.8	0.1	0.1	1.2	88.9	2.3	3.1	3.7	1.9	5.3	17.4	6.6
	Cg	>26	1	4.9	4.4	7.7	<0.8	0.1	0.1	0.6	87.4	2.4	4.1	4.6	1.3	5.2	16.8	6.3
P-630	O	0–4	1	4.2	3.8	443.9	14.3	2.8	33.8	43.6	0.3	0.1	0.4	0.2	0.1	0.5	0.7	1.0
	E	4–8	1	4.0	3.0	46.2	2.5	0.2	1.3	14.9	34.0	1.2	1.9	1.4	1.5	2.5	3.3	6.2
	Bhs	8–16	1	4.5	3.8	44.6	2.1	0.3	0.3	8.7	44.2	5.8	7.3	6.5	14.6	23.1	24.7	7.7
	Bs	16–21	1	4.8	4.1	29.0	1.3	0.3	0.2	6.9	29.2	5.6	8.6	8.4	7.5	11.4	15.8	6.6
	BC	21–26	1	5.0	4.3	18.6	0.8	0.3	0.2	1.2	82.3	4.8	7.0	5.8	3.2	6.0	10.5	7.0
	Cg	>26	1	5.1	4.6	9.6	<0.8	0.1	0.1	0.7	82.3	3.7	6.5	6.7	1.3	4.3	11.4	6.9

[a] n is the number of soil samples per horizon. Mean values are showed when n ≥ 2.
[b] pH_w and pH_k are pH values measured in distilled water and 0.1 M KCl, respectively.
[c] SB, eCEC and sAl are sum of base cations (Na, K, Ca, Mg), effective cation exchange capacity and Al saturation in cation exchange complex, respectively.
[d] Al_p (Fe_p), Al_o (Fe_o), Al_n and Fe_d: Al (Fe) extracted with Na-pyrophosphate (p), ammonium oxalate–oxalic acid (o), Al extracted with Na hydroxide (n) and Fe extracted with Na–dithionite–citrate (d), respectively.

to the C horizons (Fig. 3). This Hg_T pattern with soil depth is disrupted by the presence of subsurface peaks, which achieve values of 90–100 ng g^{-1} in the soils P220, P480, P590 and P630, and exceed 350 ng g^{-1} in the soil P340. The total Hg in the bleached E horizons of the mid-slope and upslope soils (21–33 ng g^{-1}) is similar to those in the C horizons, whereas the background values of the Hg_T (measured in the soil parent material) varied from 2 to 12 ng g^{-1}. The values of the Hg_T according to the soil horizon type, see supplementary Table S2, were statistically different, as confirmed by the Kruskal–Wallis test ($\chi^2 = 30.372$, $P = 0.000$), indicating that soil horizonation could influence the Hg_T distribution in the studied soils.

In the CCT soils, the Hg_T was highly correlated to the parameters related to the soil organic matter (total contents of C, N, and S) as well as to the Na-pyrophosphate extractable C (C_p). The sum of the exchangeable base cations (SB) and the eCEC was also well correlated with the Hg_T (Table 2). Moderate correlations were observed between the Hg_T and both the available metals (Cu_{ed} and Zn_{ed}) and the parameters related to the Al and Fe distribution (Fe_o/Fe_d, Al_p or Fe_p), whereas clay was the only particle size fraction linked to the Hg_T, although the correlation was relatively weak (Table 2).

The areal mass of the Hg_T accumulated in the uppermost 20 cm of the soils of the CCT (Hg_{TRes}) ranged from 8.8 to 13.8 mg Hg m^{-2}, being mostly stored (>70%) in the mineral layers that occur at that soil depth. Soil P220 deviated from this trend, as 60% of the Hg_{TRes} was accumulated in the O horizon. Unexpectedly, no significant correlation was found between the Hg_{TRes} and the stored organic C, although the Hg_{TRes} was highly correlated with C_p ($r = 0.814$, $P = 0.000$), the total S ($r = 0.651$, $P = 0.000$), the Al–humus complexes ($r = 0.820$, $P = 0.000$) and non-crystalline Fe ($r = 0.833$, $P = 0.000$).

The values of the Hg/C ratio in the soils of the CCT varied from 1 to 11.3 μg Hg g^{-1} C, increasing steadily with depth. In the upslope and mid-slope soils of the CCT, the subsurface peaks of the Hg/C ratio agree approximately with the Bhs and Bs horizons (supplementary Figure S1). For all the soil samples, the Hg/C ratios correlate significantly with pH_w ($r = 0.562$, $P = 0.000$), the inorganic non-crystalline Al compounds ($r = 0.625$, $P = 0.000$) and the crystalline Fe compounds ($r = 0.526$, $P = 0.000$).

3.3. Lithogenic and exogenic Hg in the soil profiles

Estimates of the lithogenic Hg (Hg_{Lit}) in the CCT soils range from 0.8 to 16.9 ng g^{-1}, with the lowest mean values present in the O horizons (approximately 2.5% Hg_T) and the highest values in the different types of B horizons, where Hg_{Lit} is 36% of the Hg_T on average (Fig. 4; supplementary Tables S3 and S4). Lithogenic Hg tends to increase with depth in the mid-slope and upslope soils (P480, P590 and P630), remaining rather uniform in soil P340 and showing variations in soil P220, where the highest values of Hg_{Lit} are found at depths between 15 cm and 60 cm. A Kruskal–Wallis test revealed that the type of soil horizon is a statistical significant factor for the values of Hg_{Lit} and the percentage of Hg_{Lit} relative to the total Hg (%Hg_{Lit}) ($\chi^2 = 15.369$, $P = 0.009$; $\chi^2 = 25.724$, $P = 0.000$, respectively).

Lithogenic Hg is negatively correlated to the total organic C ($r = -0.416$, $P = 0.004$), the total S ($r = -0.467$, $P = 0.001$),

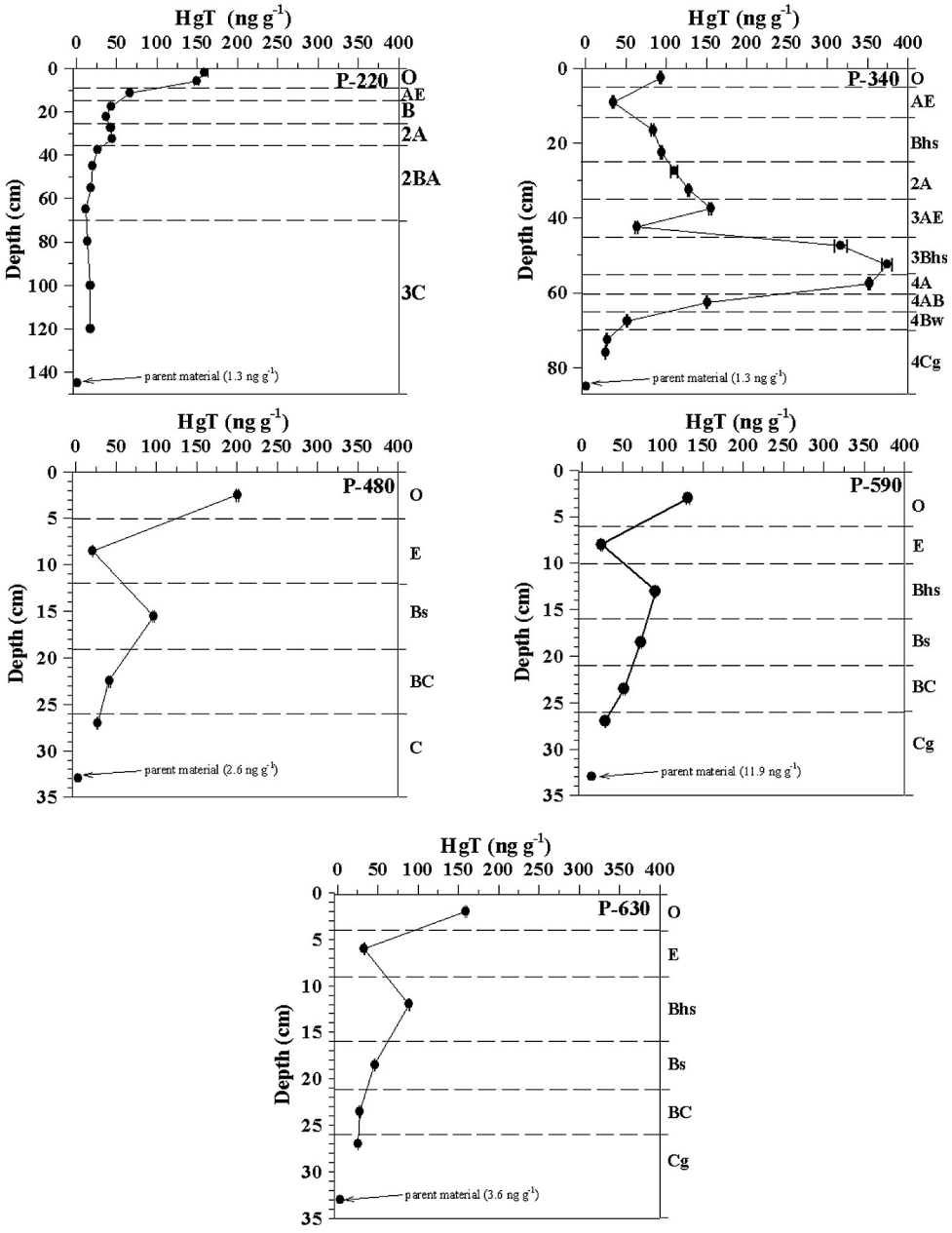

Fig. 3. Depth patterns of the total Hg (Hg_T) in the Cerro Castor toposequence soils.

and the available metals (Cu_{ed}, r = −0.563, $P = 0.000$; Zn_{ed}, r = −0.621, $P = 0.000$). Similarly, $\%Hg_{Lit}$ also correlates negatively with the same parameters that are negatively correlated to Hg_{Lit} but the correlation coefficients are above 0.800. Note the significant negative correlation between $\%Hg_{Lit}$ and Hg_T (r = −0.894, $P = 0.000$).

Table 2
Correlation coefficients (r) between the Hg_T and the soil properties of the Cerro Castor toposequence.

Hg_T	C	N	S	C_p	SB	eCEC
r	0.821** (46)	0.710** (33)	0.791** (46)	0.754** (46)	0.557** (46)	0.609** (46)
	Cu_{ed}	Zn_{ed}	Fe_o/Fe_d	Al_p	Fe_p	Clay
	0.715** (46)	0.774** (46)	0.715** (46)	0.439** (46)	0.444** (46)	0.423* (28)

The number of soil samples is in parenthesis.
** $p < 0.01$.
* $p < 0.05$.

Exogenic Hg (Hg_{Exo}) exhibits a wide range of values (3–369 ng g^{-1}; supplementary Table S3), with the highest ones occurring in the downslope soils (P220 and P340). The Hg_{Exo} pattern with soil depth is similar to the Hg_T pattern, decreasing steadily from the O and A horizons (130 and 145 ng g^{-1} as average, respectively) to the B and C horizons, where Hg_{Exo} hardly exceeds 23 ng g^{-1} (supplementary Table S4). As a percentage of the Hg_T, Hg_{Exo} in the O and A horizons' average is above 87%, whereas for the B and C horizons, this percentage is reduced to 64% (Fig. 4). Subsurface peaks of Hg_{Exo} occur in the studied soils: the soil P340 was an outlier, with values above 300 ng g^{-1} (i.e., >98% of Hg_T).

Exogenic Hg correlates significantly with the same soil parameters that are correlated with the Hg_T, for example with the total organic C, N and S (r = 0.820, $P = 0.000$; r = 0.728, $P = 0.000$; r = 0.806, $P = 0.000$, respectively) and the available metals (Cu_{ed}, r = 0.752, $P = 0.000$; Zn_{ed}, r = 0.802, $P = 0.000$). Other

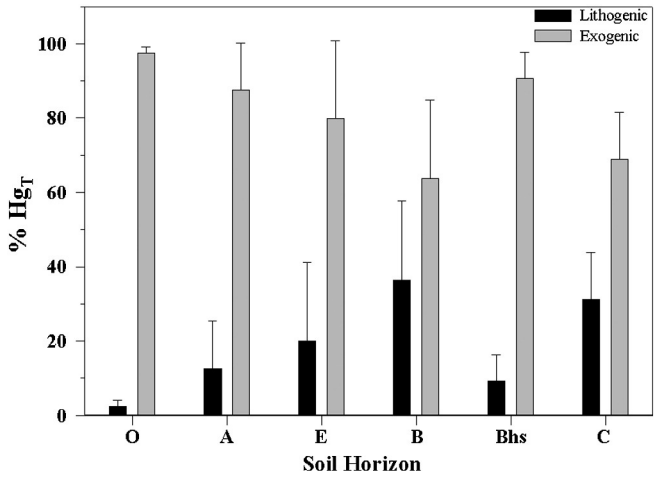

Fig. 4. Mean values (filled bars) and standard deviations (error bars) of the contribution of the lithogenic and exogenic Hg to the total Hg (Hg_T) for different soil horizons.

significant correlations for Hg_{Exo} were obtained for ratios that indicate the degree of predominance of non-crystalline forms of Al (Al_o/Al_n, r = 0.489, $P = 0.001$) and Fe (Fe_o/Fe_d, r = 0.718, $P = 0.000$) in the studied soils.

4. Discussion

The soil morphology and the chemical characteristics indicate that podzolization is the dominant process in the mid-slope and up-slope soils (P480, P590 and P630) of the CCT, as indicated by the impoverishment of organic matter and Al and Fe compounds in the bleached horizons (E horizons) and their accumulation in the illuvial (Bh, Bhs) horizons (Table 1). Different studies previously reported the presence of podzolic soils in the forested slopes of the Fuegian Andes (Colmet-Daage et al., 1991; Godagnone and Irisarri, 1990), which was attributed to a high degree of relative humidity and the production of organic acids in the O horizons (Etchevehere and Miaczynski, 1963).

In the downslope soils of the CCT, the changes in the morphological features and in the content of organic matter and the Al and Fe compounds (Table 1) seem to be the imprint of the processes of polycyclism. The occurrence of buried soils in the downslope section of the CCT results from the accumulation of colluvial material that was probably mobilized from the upslopes, a process related to the toposequence concept (Sommer and Schlichting, 1997).

The levels of the total Hg (Hg_T) in the CCT soils (12–375 ng g^{-1}) are in the order of those reported for pristine or quasi-pristine forest soils (Table 3), being consistent with the absence of anthropogenic Hg point sources in the surroundings of the study area. Moreover, in most of the soil horizons analyzed, the Hg_T values are below 100 ng g^{-1}, which is considered to be the natural background in soils (Xin and Gustin, 2007).

The high values of the Hg_T in the O horizons of the CCT soils (>94 ng g^{-1}) can result from the atmospheric deposition and litterfall, being subsequently accumulated in the organic C rich soil layers. This mechanism is supported by the correlations between the Hg_T and the total content of C, N and S (Table 2), as well as with the Cu and Zn extracted with Na_2-EDTA. It is reported that this reagent, Na_2-EDTA, extracts in podzols a fraction of metals associated to dissolved organic matter (Schlüter, 1997). Moreover, litterfall is recognized as a main transfer path of atmospheric Hg to the soil (Juillerat et al., 2012) whereas the thiol groups of soil organic matter are highly efficient in bonding to Hg (Skyllberg et al., 2006). Low Hg_T in the E horizons of the mid-slope and upslope soils (<33 ng g^{-1}) is in agreement with its potential loss by leaching due to podzolization (Johansson et al., 1991; Schuster, 1991), being favoured by the presence of dissolved organic matter (Schlüter, 1997; Yao et al., 2011) and the low pH of the soil solution (Yin et al., 1996). Both conditions are present in the E horizons of the CCT soils and could contribute to the Hg impoverishment in these horizons. Consistently, the spodic horizons of the mid-slope and upslope soils of the CCT exhibited high contents of Hg_T that coincide with an accumulation of Fe and Al compounds and humus (Fig. 3, Table 1). Significant correlations of the Hg_T exist with the Fe_o/Fe_d ratio and the metal

Table 3
Values of the total Hg (Hg_T) in the upland forest soils from published studies.

Location	Soil type[a]	Soil horizon or depth (cm)	Range or average (ng g^{-1})	Reference
Brazil	Ferralsols	Argillaceous cover	173–373	De Oliveira et al. (2001)
Brazil	Ferralsols	0–80	122–232	Do Valle et al. (2005)
Brazil	Podzols	E horizon	<25	
		Bh horizon	203–764	
Brazil	Ferralsols	0–100	88–209	Roulet et al. (1998)
Brazil	Ferralsols	0–620	5–53	Fiorentino et al. (2011)
Brazil	Ferralsols	0–80	128–150	Almeida et al. (2005)
French Guiana	Ferralsols, acrisols	0–300	9–500	Guedron et al. (2006)
French Guiana	Ferralsols, acrisols	0–300	30–800	Grimaldi et al. (2008)
French Guiana	Ferralsols, acrisols, gleysols	0–100/200	10–490	Guedron et al. (2009)
U.S.A.	Cambisols, acrisols, podzols,	0–40	7–385	Obrist et al. (2011)
U.S.A	Podzols	O + Bh + Bs	60–134	Amirbahman et al. (2004)
U.S.A.	Acrisols, cambisols	O	21–304	Obrist et al. (2009)
	n.s.	0–40	24–35	
U.S.A.	Podzols, cambisols	O + A	72–283	Juillerat et al. (2012)
Canada	Histosols	O + H	78–314	Mailman and Bodaly (2005)
Canada	Chernozems	0–100 (averaged)	10–62	Dudas and Pawluk (1976)
Canada	Luvisols	0–135 (averaged)	10–146	
Germany	Podzols	0–60	20–500	Schwesig et al. (1999)
Germany	Podzols, cambisols	0–60/75	20–500	Schwesig and Matzner (2000)
Sweden	Podzols	O + A/E + Bhs + C	37–268	Larssen et al. (2008)
Sweden	Podzols, regosols	O	320	Alriksson (2001)
		B	43	
France	Podzols	0–80	16–399	Hissler and Probst (2006)
U.K.	n.s.	0–15	115–389	Tipping et al. (2011)
China	Cambisols, podzols	0–20	10–270	Fu et al. (2010)

[a] According to FAO-WRBSR unless not specified (n.s.).

(Al, Fe)–humus complexes (Al_p, Fe_p) in the CCT soils (Table 2), indicating that these soil compounds are involved in the retention of the mobilized Hg, thereby contributing to the Hg enrichment observed in the illuvial horizons of the CCT soils. Similar results were also reported in studies on the fate of Hg in podzolic soils (Alriksson, 2001; Do Valle et al., 2005; Larssen et al., 2008; Nóvoa-Muñoz et al., 2008; Roulet et al., 1998; Schwesig and Matzner, 2000). Deeper in the soil, the low values of Hg_T in the C horizons of the CCT are in agreement with its low content in the parent material, far from the average of 40 ng g^{-1} for the continental crust (Wedepohl, 1995). In addition, the climatic conditions do not favour the transference of Hg to the soil through mineral weathering, conversely to that reported for tropical soils (De Oliveira et al., 2001; Roulet et al., 1998).

In the downslope soils of the CCT (P220 and P340), the subsurface peaks of the Hg_T are mostly associated with the buried A horizons (Fig. 3), probably due to its exposure to atmospheric deposition when they occupied the soil surface, as was recently considered by Obrist et al. (2011) to justify the Hg enrichment in the uppermost horizons of forest soils. This Hg accumulation in the buried A horizons can also result from the loss of C and N mass during organic matter mineralization with a simultaneous conservation of the Hg mass (Demers et al., 2007; Obrist et al., 2009). The downward transport of Hg due to podzolization in present and buried soil cycles and the lateral component of the drainage flux could explain the exceptionally high values of Hg_T in the buried soil horizons compared to similar horizons in present soils (Fig. 3).

Pedogenetic processes seem to largely control the Hg_T distribution in the soils of the CCT, either mobilizing Hg due to the intrinsic pedogenetic process or through its interaction with the soil compounds that originated during soil formation. Thus, the podzolization could be responsible for the Hg distribution in the mid-slope and upslope soils, whereas for the downslope soils, an overlapping of podzolization and polycyclism determines the Hg_T pattern with depth. These processes could explain the statistical significant differences in the Hg_T as a function of soil horizons, a fact already mentioned for podzolic forest soils (Amirbahman et al., 2004).

The Hg_T stored (Hg_{TRes}) in the uppermost 20 cm of the soils of the CCT is comparable to the values reported in the literature (supplementary Table S5). In spite of the scatter in the data, the Hg_{TRes} strongly depends on the soil thickness and bulk density used for the estimation of the stored Hg_T (Grigal, 2003; Larssen et al., 2008). Thus, Tipping et al. (2011) considered that the bulk density is primarily responsible for the greater amount of Hg stored in the mineral horizons than in the organic horizons, which is similar to that found in the CCT soils. The predominance of the mineral horizons versus the organic horizons as the main soil Hg reservoir is recurrently found in the literature (Amirbahman et al., 2004; Juillerat et al., 2012; Nóvoa-Muñoz et al., 2008; Obrist, 2012; Roulet et al., 1998; Schwesig and Matzner, 2000; Schwesig et al., 1999).

As podzolization and polycyclic processes in the soils of CCT could be responsible for the Hg enrichment of the buried A and Bhs horizons, their contribution to the Hg_{TRes} should not be neglected, or else the soil Hg inventory could be underestimated. This suggestion is supported by Schwesig et al. (1999), who considered that a proportion of the Hg_{TRes} in the mineral soil could result from the downward Hg transport during podzolization. The thickening of the O horizon in the lowest altitude soil (P220), possibly a result of an increase of the annual litterfall supply compared to the highest altitudes (Barrera et al., 2000), could justify the greater contribution of this organic horizon to the Hg storage calculated for this soil. This altitude dependence is consistent with studies that consider Hg accumulation to occur mainly in the surface soil horizons (Obrist, 2012; Obrist et al., 2009).

The lack of correlation between the Hg_{TRes} and the total C content in the CCT soils could be attributed to the distinctive degree of humification of the soil organic matter in the organic and mineral soil layers, which influences the ability of organic matter to bind to Hg. The role of humified organic matter in the preferential Hg storage in the uppermost soil layers is consistent with the significant correlations between the Hg_{TRes} and the Al–humus complexes, the total S, the Na-pyrophosphate C (C_p) and the non-crystalline Fe, as most of these soil compounds require the presence of humified organic matter to occur. However, other studies reported a close correlation between the total C and Hg_{TRes} (Juillerat et al., 2012; Obrist et al., 2009).

The Hg/C ratio, considered a more suitable approach to asses Hg distribution with soil depth (Obrist et al., 2011; Tipping et al., 2010), indicates values for the CCT soils on the order of the ranges of 0.3–1.1 and 1.4–3.2 μg Hg g^{-1} C reported for the O and A horizons, respectively, of the forest soils in the Unites States and in Poland (Juillerat et al., 2012; Obrist et al., 2009, 2011). The trend of the Hg/C ratio with depth in the CCT soils matches approximately with the C_p/C ratio, which is considered to be an estimate of the degree of soil organic matter humification (supplementary Figure S1). The humified organic matter is known to be highly efficient in retaining Hg (Amirbahman et al., 2004), as it promotes the Hg mobilization through organically-complexed species (Åkerblom et al., 2008) and exhibits a lower loss of Hg than C during organic matter decomposition (Grigal, 2003). Recently, the degree of organic matter humification represented by the C/N ratio was also demonstrated to be negatively correlated to the Hg/C ratio (Obrist et al., 2011). The peaks of the Hg/C ratio in illuvial horizons (Bhs, Bs) of the CCT soils could be attributed to the presence of non-crystalline Al or crystalline Fe compounds, as was also suggested by Amirbahman et al. (2004).

Some controversy could arise from these estimates of lithogenic Hg (Hg_{Lit}) and exogenic Hg (Hg_{Exo}), because Ti mobilization as organic matter complexes was found in podzolic soils (Skjemstad et al., 1992), but other studies considered that Ti is not subjected to downward translocation in podzols (Berrow et al., 1978). However, estimates of Hg_{Lit} and Hg_{Exo} are consistent with the expectations according to the soil processes in the CCT and the potential Hg sources in the study area. The values of lithogenic and exogenic Hg indicate that the atmosphere is the main source of Hg to CCT soils (Fig. 4). The predominance of Hg_{Exo} in the O and A horizons of the CCT soils, up to 87% of the Hg_T, is similar to the 75% reported for the upper metre of tropical soils (Grimaldi et al., 2008); these observations are reasonable, because the O and A horizons are the first soil layers that interact with atmospheric deposited Hg or receive Hg through litterfall. Moreover, soil organic matter that occurs in these soil layers contributes to an efficient retention of the deposited Hg. This retention could justify the significant correlations between Hg_{Exo} and some parameters associated to the soil organic matter, which is similar to the characteristics reported for the uppermost layers of volcanic soils (Peña-Rodríguez et al., 2012). The comparison between podzolic soils and volcanic soils is due to they share, in addition to organic matter, other variable charge compounds such as Al (Fe)–humus complexes and poorly ordered Al and Fe oxyhydroxide compounds (Parfitt, 1980) which are very active in terms of Hg retention.

The lithogenic Hg values in the CCT soils (1–17 ng g^{-1}) are slightly lower than the values of 30 ng g^{-1} estimated for soils from France and French Guiana (Guedron et al., 2006; Hissler and Probst, 2006). In the deeper soil horizons (B and C), Hg_{Lit} became more important, possibly as a result of the influence of the soil parent material and a less probable contribution of Hg_{Exo} (Fig. 4). This proposed that the influence of the soil parent material is supported by the similarity of the values of Hg_{Lit} in these horizons and the Hg_T values of the soil parent material, an explanation already considered by Hissler and Probst (2006) in a similar case.

The high values of Hg_{Lit} in the deeper horizons of P220 of up to 30% of the Hg_T (supplementary Table S3) could be attributed to the mineral matter input that occurs during polycyclic events. The peaks of Hg_{Exo} in the buried A horizons (P220 and P340) can be explained as a result of the heritage of these horizons, when they were at the soil surface, or due to the accumulation of the Hg mobilized downward. Regarding the Hg_{Exo} peaks in the Bhs or Bs horizons (P340, P480, P590 and P630), they probably result from Hg mobilization from the overlaying horizons and the subsequent retention by Al and Fe compounds (i.e., podzolization). Significant correlations between Hg_{Exo} and the ratios

of the crystalline/non-crystalline compounds of Al and Fe (Al_o/Al_n and Fe_o/Fe_d) support this hypothesis, which is also consistent with the findings that consider that the Hg_{Exo} depth pattern depends on the transfer processes and the abundance of the soil compounds able to retain Hg, such as organic matter or Al and Fe oxyhydroxides (Grimaldi et al., 2008; Guedron et al., 2006, 2009).

5. Conclusions

The vertical distribution of the total Hg in the soils of the Cerro Castor toposequence is consistent with the podzolization in the up-slope and mid-slope soils (P480, P590 and P630) and with the polycyclic events in the downslope soils (P220 and P340). Concurrently, the Hg_T is closely related to the soil organic matter (total C, N, S, C_p), the metal (Al, Fe)–humus complexes and the non-crystalline Al and Fe compounds.

The degree of humification of the soil organic matter could be responsible for the greater Hg storage ability exhibited by the mineral horizons over that exhibited by the organic horizons in the upper 20 cm of the CCT soils. This hypothesis is supported by the close correlations of the Hg_{TRes} with the Al–humus complexes and the Na-pyrophosphate extracted C (C_p). The subsurface peaks of the Hg_T in the illuvial (Bhs, Bs) and buried A horizons should not be neglected when a comprehensive pool of the total Hg is estimated in the CCT soils. Similar depth patterns of the Hg/C and C/C_p ratios also resemble the role of humified organic matter in the retention of Hg in the soil.

The use of Ti as reference element results in consistent estimates of Hg_{Exo} and Hg_{Lit} in the CCT soils, with a predominance of Hg_{Exo} in the uppermost soil layers, suggesting the domain of an atmospheric source and an expected significance of Hg_{Lit} in the deeper soil horizons (B and C). The peaks of Hg_{Exo} in the illuvial Bhs and Bs horizons are probably due to Hg mobilization during podzolization, whereas the high values of Hg_{Exo} in the buried A horizons could represent a legacy effect due to its exposure to atmospheric inputs in the past as well as a contribution of the lateral component of the drainage flux which favours the mobilization of Hg bound to organic matter.

The influence of pedogenetic processes in the Hg distribution in the CCT soils should also be viewed from an environmental perspective. The uppermost layers of the CCT soils serve as a fence that temporarily prevents Hg mobilization, whereas the illuvial (Bs and Bhs) and buried A horizons can act as a secondary safety mechanism, immobilizing Hg favoured by the accumulation in the deep horizons of organic matter, metal (Al, Fe)–humus complexes and Al and Fe oxyhydroxides that result from the podzolization and polycyclism processes. Thus, the arrival of Hg to stream waters is delayed, thereby diminishing the potential transformation of ionic Hg (mainly Hg^{2+}) to highly toxic methyl mercury (MeHg) in the lowland areas, which are mostly covered by peatlands.

Acknowledgements

This research was partially funded by Fundación BBVA (Project BIOCON05/119-CARBOCLIM) and by the Project PICTO FORESTAL (Resol. ANPCyT 225/07, cod. 36861). The stays of S. Peña-Rodríguez and J. C. Nóvoa-Muñoz in Ushuaia (Argentina) was enabled by the financial support of CIA3 which was granted by FEDER founds through the programme of Consolidation and Arrangement of Research Units from Consellería de Educación (Xunta de Galicia). The stay of X. Pontevedra-Pombal in Ushuaia (Argentina) was funded by the Department of Innovation and Industry (Xunta de Galicia) co-financed by the Integrated Operational Programme for Galicia of EU.

Appendix A. Supplementary data

Supplementary data to this article can be found online at http://dx.doi.org/10.1016/j.geoderma.2014.04.040.

References

Åkerblom, S., Meili, M., Bringmark, L., Johansson, K., Kleja, D.B., Bergkvist, B., 2008. Partitioning of Hg between solid and dissolved organic matter in the humus layer of boreal forests. Water Air Soil Pollut. 189, 239–252.
Almeida, M.D., Lacerda, L.D., Bastos, W.R., Herrmann, J.C., 2005. Mercury loss from soils following conversion from forest to pasture in Rondônia, Western Amazon, Brazil. Environ. Pollut. 137, 179–186.
Alriksson, A., 2001. Regional variability of Cd, Hg, Pb and C concentrations in different horizons of Swedish forest soils. Water Air Soil Pollut. Focus 1, 325–341.
Amirbahman, A., Ruck, P.L., Fernandez, I.J., Haines, T.A., Kahl, J.S., 2004. The effect of fire on mercury cycling in the soils of forested watersheds: Acadia National Park, Maine, U.S.A. Water Air Soil Pollut. 152, 313–331.
Bargagli, R., Monaci, F., Bucci, C., 2007. Environmental biogeochemistry of mercury in Antarctic ecosystems. Soil Biol. Biochem. 39, 352–360.
Barrera, M.D., Frangi, J.L., Richter, L.L., Perdomo, M.H., Pinedo, L.B., 2000. Structural and functional changes in *Nothofagus pumilio* forests along an altitudinal gradient in Tierra del Fuego, Argentina. J. Veg. Sci. 11, 179–188.
Bascopé, J., 2010. El oro y la vida salvaje en Tierra del Fuego, 1880–1914. Magallania 38, 5–26.
Berrow, M.L., Wilson, M.J., Reaves, G.A., 1978. Origin of extractable titanium and vanadium in the a horizons of Scottish podzols. Geoderma 21, 89–103.
Bertsch, P.M., Bloom, P.R., 1996. Aluminium. Anonymous Methods of Soil Analysis. Part 3—Chemical Methods. SSSA, Wisconsin, EE.UU, pp. 517–550.
Clarkson, T.W., Magos, L., 2006. The toxicology of mercury and its chemical compounds. Crit. Rev. Toxicol. 36, 609–662.
Colmet-Daage, F., Irisarri, M., Lanciotti, M., 1991. Los Suelos Ácidos Con Al Activo y Montmorillonita, Illita, Vermiculita e Interestratificados De Tierra Del Fuego, Argentina y Chile. INTA-ORSTOM. Publicación de la Universidad Nacional de Comahue.
De Oliveira, S.M.B., Melfi, A.J., Fostier, A.H., Forti, M.C., Fávaro, D.I.T., Boulet, R., 2001. Soils as an important sink for mercury in the Amazon. Water Air Soil Pollut. 126, 321–337.
Demers, J.D., Driscoll, C.T., Fahey, T.J., Yavitt, J.B., 2007. Mercury cycling in litter and soil in different forest types in the Adirondack region, New York, USA. Ecol. Appl. 17, 1341–1351.
Do Valle, C.M., Santana, G.P., Augusti, R., Egreja Filho, F.B., Windmöller, C.C., 2005. Speciation and quantification of mercury in oxisol, ultisol, and spodosol from Amazon (Manaus, Brazil). Chemosphere 58, 779–792.
Dudas, M.J., Pawluk, S., 1976. The nature of mercury in chernozemic and luvisolic soils in Alberta. Can. J. Soil Sci. 56, 413–423.
Elliot, A.C., Woodward, W.A., 2007. Statistical Analysis. Quick Reference Guidebook With SPSS Examples. , SAGE Publications, Inc, Thousand Oaks, CA.
Etchevehere, P.H., Miaczynski, C.R., 1963. Los Suelos De Tierra Del Fuego. Instituto de Suelos y Agrotecnia. , INTA, Buenos Aires, Argentina.
Fiorentino, J.C., Enzweiler, J., Angélica, R.S., 2011. Geochemistry of mercury along a soil profile compared to other elements and to the parental rock: evidence of external input. Water Air Soil Pollut. 221, 63–75.
Fu, X., Feng, X., Zhu, W., Rothenberg, S., Yao, H., Zhang, H., 2010. Elevated atmospheric deposition and dynamics of mercury in a remote upland forest of southwestern China. Environ. Pollut. 158, 2324–2333.
García-Rodeja, E., Nóvoa Muñoz, J.C., Pontevedra, X., Martínez-Cortizas, A., Buurman, P., 2007. Aluminium and iron fractionation of European volcanic soils by selective dissolution techniques. In: Arnalds, O., Bartoli, F., Buurman, P., Oskarsson, H., Stoops, G., García-Rodeja, E. (Eds.), Soils of Volcanic Regions in Europe. Springer, Berlin, pp. 325–351.
Glodek, A., Pacyna, J.M., 2009. Mercury emission from coal-fired power plants in Poland. Atmos. Environ. 43, 5668–5673.
Godagnone, R., Irisarri, J., 1990. Mapa de suelos del Territorio Nacional de Tierra del Fuego. In: Moscatelli, G. (Ed.), Atlas De Suelos De La República Argentina. SAGyP-INTA-Proyecto PNUD, pp. 615–641.
Grigal, D.F., 2003. Mercury sequestration in forests and peatlands: a review. J. Environ. Qual. 32, 393–405.
Grimaldi, C., Grimaldi, M., Guedron, S., 2008. Mercury distribution in tropical soil profiles related to origin of mercury and soil processes. Sci. Total Environ. 401, 121–129.
Guedron, S., Grimaldi, C., Chauvel, C., Spadini, L., Grimaldi, M., 2006. Weathering versus atmospheric contributions to mercury concentrations in French Guiana soils. Appl. Geochem. 21, 2010–2022.
Guedron, S., Grangeon, S., Lanson, B., Grimaldi, M., 2009. Mercury speciation in a tropical soil association; consequence of gold mining on Hg distribution in French Guiana. Geoderma 153, 331–346.
Gustin, M.S., Engle, M., Ericksen, J., Lyman, S., Stamenkovic, J., Xin, M., 2006. Mercury exchange between the atmosphere and low mercury containing substrates. Appl. Geochem. 21, 1913–1923.
Gustin, M.S., Lindberg, S.E., Weisberg, P.J., 2008. An update on the natural sources and sinks of atmospheric mercury. Appl. Geochem. 23, 482–493.
Hermanns, Y.M., Biester, H., 2011. A Holocene record of mercury accumulation in a pristine lake in southernmost South America (53° S) — climatic and environmental drivers. Biogeosci. Discuss. 8, 6555–6588.
Hissler, C., Probst, J., 2006. Impact of mercury atmospheric deposition on soils and streams in a mountainous catchment (Vosges, France) polluted by chlor-alkali industrial activity: the important trapping role of the organic matter. Sci. Total Environ. 361, 163–178.
Johansson, K., Aastrup, M., Andersson, A., Bringmark, L., Iverfeldt, A., 1991. Mercury is Swedish forest soils and waters — assessment of critical load. Water Air Soil Pollut. 56, 267–281.
Juillerat, J.I., Ross, D.S., Bank, M.S., 2012. Mercury in litterfall and upper soil horizons in forested ecosystems in Vermont, USA. Environ. Toxicol. Chem. 31, 1720–1729.

Lakenen, E., Ervio, R.A., 1971. A comparison of eight extractants for the determination of plant-available micronutrients in soils. Acta Agralia Fenn. 123, 223–232.
Larssen, T., de Wit, H.A., Wiker, M., Halse, K., 2008. Mercury budget of a small forested boreal catchment in southeast Norway. Sci. Total Environ. 404, 290–296.
Mailman, M., Bodaly, R.A., 2005. Total mercury, methyl mercury, and carbon in fresh and burned plants and soil in Northwestern Ontario. Environ. Pollut. 138, 161–166.
Mason, R.P., Sheu, G.-., 2002. Role of the ocean in the global mercury cycle. Glob. Biogeochem. Cycles 16, 40–41.
Meili, M., 1991. The coupling of mercury and organic matter in the biogeochemical cycle — towards a mechanistic model for the boreal forest zone. Water Air Soil Pollut. 56, 333–347.
Mitchell, C.P.J., Branfireun, B.A., Kolka, R.K., 2008. Total mercury and methylmercury dynamics in upland–peatland watersheds during snowmelt. Biogeochemistry 90, 225–241.
Munthe, J., Hultberg, H., Iverfeldt, A., 1995. Mechanisms of deposition of methylmercury and mercury to coniferous forests. Water Air Soil Pollut. 80, 363–371.
Nóvoa-Muñoz, J.C., Pontevedra-Pombal, X., Martínez-Cortizas, A., García-Rodeja Gayoso, E., 2008. Mercury accumulation in upland acid forest ecosystems nearby a coal-fired power-plant in Southwest Europe (Galicia, NW Spain). Sci. Total Environ. 394, 303–312.
Obrist, D., 2012. Mercury distribution across 14 U.S. forests. Part II: patterns of methyl mercury concentrations and areal mass of total and methyl mercury. Environ. Sci. Technol. 46, 5921–5930.
Obrist, D., Johnson, D.W., Lindberg, S.E., 2009. Mercury concentrations and pools in four Sierra Nevada forest sites, and relationships to organic carbon and nitrogen. Biogeosciences 6, 765–777.
Obrist, D., Johnson, D.W., Lindberg, S.E., Luo, Y., Hararuk, O., Bracho, R., Battles, J.J., Dail, D. B., Edmonds, R.L., Monson, R.K., Ollinger, S.V., Pallardy, S.G., Pregitzer, K.S., Todd, D.E., 2011. Mercury distribution across 14 U.S. forests. Part I: spatial patterns of concentrations in biomass, litter, and soils. Environ. Sci. Technol. 45, 3974–3981.
Olivero, E.B., Martinioni, D.R., 2001. A review of the geology of the Argentinian Fuegian Andes. J. S. Am. Earth Sci. 14, 175–188.
Parfitt, R.L., 1980. Chemical properties of variable change soils. In: Theng, B.K.G. (Ed.), Soils With Variable Charge. New Zealand Society of Soil Science, Palmerston North, New Zealand, pp. 167–194.
Peech, M., Alexander, L.T., Dean, L.A., Reed, J.F., 1947. Methods of Soil Analysis for Soil Fertility Investigations. , US. Department of Agriculture, Washington, Estados Unidos.
Peña-Rodríguez, S., Pontevedra-Pombal, X., Fernández-Calviño, D., Taboada, T., Arias-Estévez, M., Martínez-Cortizas, A., Nóvoa-Muñoz, J.C., García-Rodeja, E., 2012. Mercury content in volcanic soils across Europe and its relationship with soil properties. J. Soils Sediments 12, 542–555.
Rothenberg, S.E., McKee, L., Gilbreath, A., Yee, D., Connor, M., Fu, X., 2010. Wet deposition of mercury within the vicinity of a cement plant before and during cement plant maintenance. Atmos. Environ. 44, 1255–1262.
Roulet, M., Lucotte, M., Saint-Aubin, A., Tran, S., Rhéault, I., Farella, N., De Jesus Da Silva, E., Dezencourt, J., Sousa Passos, C., Santos Soares, G., Guimarães, J.-.D., Mergler, D., Amorim, M., 1998. The geochemistry of mercury in central Amazonian soils developed on the Alter-do-Chao formation of the lower Tapajos River Valley, Para state, Brazil. Sci. Total Environ. 223, 1–24.
Schlüter, K., 1997. Sorption of inorganic mercury and monomethyl mercury in an iron–humus podzol soil of southern Norway studied by batch experiments. Environ. Geol. 30, 266–279.
Schroeder, W.H., Munthe, J., 1998. Atmospheric mercury — an overview. Atmos. Environ. 32, 809–822.
Schuster, E., 1991. The behavior of mercury in the soil with special emphasis on complexation and adsorption processes — a review of the literature. Water Air Soil Pollut. 56, 667–680.
Schwesig, D., Matzner, E., 2000. Pools and fluxes of mercury and methylmercury in two forested catchments in Germany. Sci. Total Environ. 260, 213–223.
Schwesig, D., Ilgen, G., Matzner, E., 1999. Mercury and methylmercury in upland and wetland acid forest soils of a watershed in Ne-Bavaria, Germany. Water Air Soil Pollut. 113, 141–154.
Skjemstad, J.O., Fitzpatrick, R.W., Zarcinas, B.A., Thompson, C.H., 1992. Genesis of podzols on coastal dunes in southern Queensland. II. Geochemistry and forms of elements as deduced from various soil extraction procedures. Aust. J. Soil Res. 30, 615–644.
Skyllberg, U., Bloom, P.R., Qian, J., Lin, C.-., Bleam, W.F., 2006. Complexation of mercury(II) in soil organic matter: EXAFS evidence for linear two-coordination with reduced sulfur groups. Environ. Sci. Technol. 40, 4174–4180.
Sommer, M., Schlichting, E., 1997. Archetypes of catenas in respect to matter — a concept for structuring and grouping catenas. Geoderma 76, 1–33.
St. Louis, V.L., Rudd, J.W.M., Kelly, C.A., Hall, B.D., Rolfhus, K.R., Scott, K.J., Lindberg, S.E., Dong, W., 2001. Importance of the forest canopy to fluxes of methyl mercury and total mercury to boreal ecosystems. Environ. Sci. Technol. 35, 3089–3098.
Tipping, E., Lofts, S., Hooper, H., Frey, B., Spurgeon, D., Svendsen, C., 2010. Critical limits for Hg(II) in soils, derived from chronic toxicity data. Environ. Pollut. 158, 2465–2471.
Tipping, E., Poskitt, J.M., Lawlor, A.J., Wadsworth, R.A., Norris, D.A., Hall, J.R., 2011. Mercury in United Kingdom topsoils; concentrations, pools, and critical limit exceedances. Environ. Pollut. 159, 3721–3729.
Wedepohl, K.H., 1995. The composition of the continental crust. Geochim. Cosmochim. Acta 59, 1217–1232.
Xin, M., Gustin, M.S., 2007. Gaseous elemental mercury exchange with low mercury containing soils: investigation of controlling factors. Appl. Geochem. 22, 1451–1466.
Yao, A., Qiu, R., Qing, C., Mu, S., Reardon, E.J., 2011. Effects of humus on the environmental activity of mineral-bound Hg: influence on Hg plant uptake. J. Soils Sediments 11, 959–967.
Yin, Y., Allen, H.E., Li, Y., Huang, C.P., Sanders, P.F., 1996. Adsorption of mercury(II) by soil: effects of pH, chloride, and organic matter. J. Environ. Qual. 25, 837–844.